Effects of Bi³⁺ Ion-Doped on the Microstructure and Photoluminescence of La0.97Pr0.03VO4 Phosphor

Hao-Long Chen[1], Hung-Rung Shih[2], Sean Wu[3], Yee-Shin Chang[4,*]

[1]Department of Mechanical Engineering, National Pingtung University of Science and Technology, Pingtung, Taiwan

[2]Department of Mechanical and Computer-Aided Engineering, National Formosa University, Yunlin, Taiwan

[3]Department of Digital Game and Animation Design, Tungfang Design University, Kaohsiung, Taiwan

[4]Department of Electronic Engineering, National Formosa University, Yunlin, Taiwan

Abstract

The objective of this paper is to enhance the emission intensity of La0.97Pr0.03VO4 single-phased white light emitting phosphor. The Bi³⁺ ion-doped La0.97Pr0.03VO4 single-phased white light emitting phosphors are synthesized using a sol-gel method. The structure and photoluminescence properties of (La0.97-yBiy)Pr0.03VO4 (y = 0-0.05) phosphor are also examined. The XRD results show that the structure of La0.97Pr0.03VO4 phosphors with different concentrations of Bi³⁺ ion doping keeps the monoclinic structure. The SEM results show that the phosphor particles become smoother when the Bi³⁺ ion is doped. The excitation band for La0.97Pr0.03VO4 phosphor exhibits a blue shift from 320 nm to 308 nm as the Bi³⁺ ion contents are increased. The maximum emission intensity is achieved for a Bi³⁺ ion content of 0.5 mol%, which is about 30% greater than that with no Bi³⁺ ion doped. The CIE chromaticity coordinates are all located in the near white light region for different Bi³⁺ ion-doped La0.97Pr0.03VO4 phosphors.

1. Introduction

Rare-earth ion-doped oxide-based phosphors have been the subject of many studies because of their excellent optical properties [1]. They are widely used in various optical devices, such as Plasma Display Panels (PDPs), Field Emission Displays (FEDs), and Light-Emitting Diodes (LEDs) [2]. White Light-Emitting Diodes (w-LED) perform better than traditional incandescent and fluorescent lamps [3-4]. A w-LED is produced using a blue InGaN chip with commercial $Y_3Al_5O_{12}$:Ce^{3+} (YAG:Ce) yellow-emitting phosphors [5-6]. Unfortunately, this combination yields a low color-rendering index because there is no red-light-emitting component [7-8]. Recent advances in single-phased white light emitting phosphors, [9-10] have many applications for w-LEDs.

For the vanadate groups, lanthanum orthovanadates ($LaVO_4$) has many applications. Lanthanum orthovanadates have two types of crystal structure: monoclinic (m-) monazite and tetragonal (t-) zircon [11-12]. Monoclinic $LaVO_4$ is the thermodynamically stable state, and m-monazite based materials are used in laser host materials [13], solar cells [14], and thin film phosphors [15]. A previous study results show that the CIE chromaticity coordinate is located in the white light region with x = 0.388 and y = 0.367 when the m-monazite $LaVO_4$ is doped with Pr^{3+} ion at a concentration of 3 mol% produced using a sol-gel method [16].

---

* Corresponding author. E-mail address: yeeshin@nfu.edu.tw

The sol-gel method requires a low synthesis temperature, achieves higher purity, mixes activators well, and produces nano-scale particle powders [17-18]. Many studies enhance the photoluminescence properties of phosphors and improve the particle morphology by flux addition or by doping with different radius ions [19-20]. Doping with different radius ions is the simplest and most effective method. For example, the emission intensity for $BaLa_{1.5}Eu_{0.5}ZnO_5$ phosphors with 70 mol% Ba^{2+} ion substituted by Sr^{2+} ion is 62% greater than that for phosphors with no Sr^{2+} ions, and 33% greater than that for commercial red sulfide phosphors $[ZnS:(Mn^{2+}, Te^{2+})]$ [20].

In order to increase the emission intensity of $La_{0.97}Pr_{0.03}VO_4$ phosphor, the Bi^{3+} ion-doped $La_{0.97}Pr_{0.03}VO_4$ phosphors are synthesized using a sol-gel method in this study. The crystal structure, surface morphologies, and the photoluminescence properties of Bi^{3+} ion-doped $La_{0.97}Pr_{0.03}VO_4$ phosphors are also determined.

2. Experimental Method

$(La_{0.97-y}Bi_y)Pr_{0.03}VO_4$ (y = 0-0.05) phosphors are synthesized using a sol-gel method with the raw materials of ammonium metavanadate (NH_4VO_3), lanthanum acetate $[La(CH_3CO_2)_3]$, and praseodymium acetate $[Pr(CH_3CO_2)_3]$. These starting materials with a purity of 99.99% are supplied by Aldrich Chemical Company, INC. A solution of ammonia (NH_4OH) is added to the NH_4VO_3 solution to accelerate dissolution, and the lanthanum acetate and praseodymium acetate are separately dissolved in deionized water. Citric Acid is used as the raw material and mixed using DI water as a solvent. After mixing, the solution is stirred and heated at 120°C for 5 h, and then is placed in an oven at 120°C for drying. Finally, the powders are calcined in a furnace at 950°C for 6 h in air using a heating rate of 4°C /min.

The structural characterization of these samples is analyzed by X-ray powder diffraction (XRD, Bruker axs), using CuKα radiation with a source power of 30 kV and a current of 20 mA. The morphologies of the phosphor powder are determined using the scanning electron microscopy (FE-SEM, Hitachi S4800-I). A Hitachi U-3010 UV visible spectrophotometer is used to measure the optical absorption behavior of the $(La_{0.97-y}Bi_y)Pr_{0.03}VO_4$ phosphor. The samples are placed inside a closed quartz glass and measured from 200 to 700 nm at room temperature. Both of the excitation and the emission spectra for the phosphors are measured at room temperature using a Hitachi F-7000 fluorescence spectrophotometer with a 150 W xenon arc lamp as the excitation source.

3. Results and Discussion

The surface morphologies of the phosphor particles must be as smooth as possible, with a high degree of crystallization, to ensure good photoluminescence efficiency.

3.1. XRD and FE-SEM characterization

The X-ray powder diffraction patterns for $(La_{0.97-y}Bi_y)Pr_{0.03}VO_4$ (y = 0-0.05) phosphors calcined at 950°C in air for 6 h using a sol-gel method are shown in Fig. 1. The crystal structure of different concentrations of Bi^{3+} ion-doped $La_{0.97}Pr_{0.03}VO_4$ phosphors is monoclinic for $LaVO_4$ (JCPDS No. 70-2392). There is no secondary phase if the Bi^{3+} ion concentration is increased because the Bi^{3+} ion (1.03Å) and La^{3+} ion have similar radii (1.032Å) [21] and the same valence. Therefore, a solid solution is formed when the La^{3+} ion is substituted by Bi^{3+} ion in the host material.

Fig. 2 shows the FE-SEM surface morphologies of $(La_{0.97-y}Bi_y)Pr_{0.03}VO_4$ (y = 0-0.05) phosphors calcined at 950°C for 6 h in air. The particle shapes are irregular and there are aggregations. For the Bi^{3+} ion concentration is 0.5 mol%, the particles become smooth, granular, and more uniform in size. A liquid-phase sintering behavior is observed when the Bi^{3+} ion concentration is more than 0.5 mol% because the Bi^{3+} ion oxidizes with O^{2-} ion to form Bi_2O_3 during the calcination process in air. Bi_2O_3 has a lower melting point of 815°C and acts as a flux in the calcination process, so the phosphor particles coagulate

due to the surface tension of the liquid when the fluxes melt. The melted fluxes also enable the phosphor particles to slide and rotate easier, so there is greater particle-particle contact and particle growth increases [22]. When the fluxes melt sufficiently, the liquid-phase sintering leads metal oxide particles to aggregate.
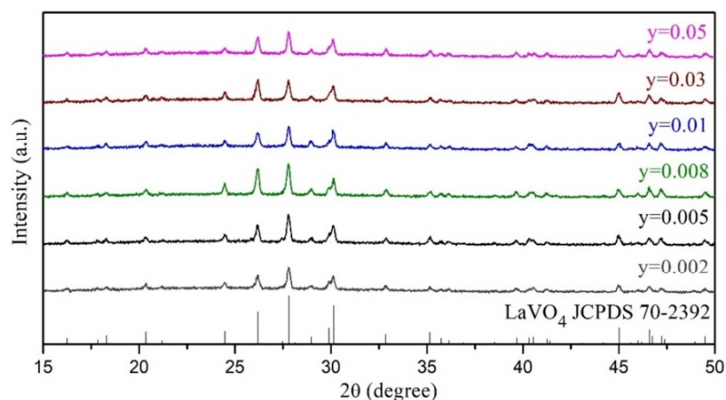
Fig. 1 The X-ray diffraction patterns of $(La_{0.97-y}Bi_y)Pr_{0.03}VO_4$ phosphors calcined at 950°C for 6 h in air

(a) 0 mol%

(b) 0.2 mol%

(c) 0.5 mol%

(d) 1 mol%
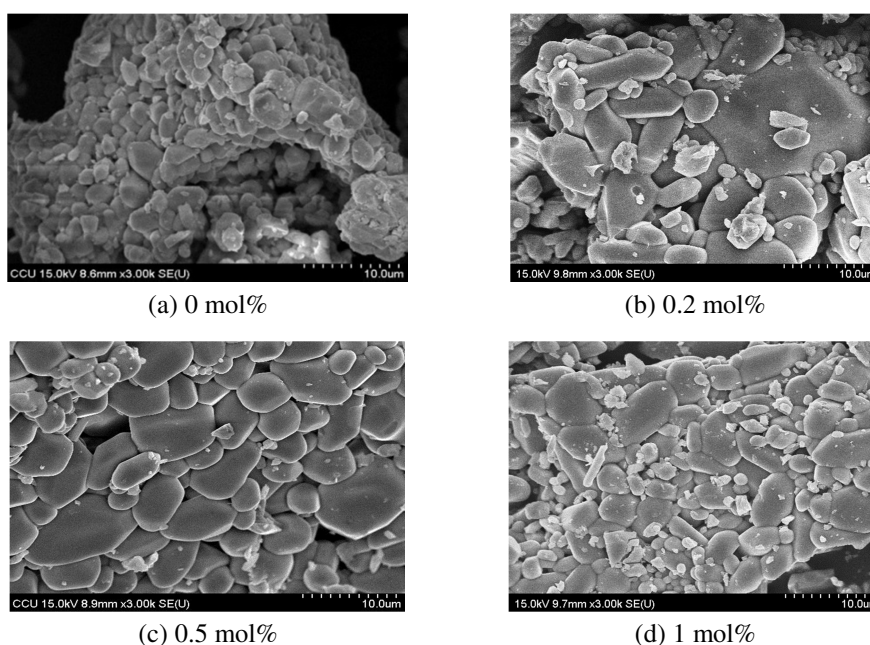
Fig. 2 FE-SEM micrographs of $La_{0.97}Pr_{0.03}VO_4$ doped with various Bi^{3+} ion concentrations calcined at 950°C for 6 h in air

3.2. Luminescence properties

The absorption spectra of $(La_{0.97-y}Bi_y)Pr_{0.03}VO_4$ phosphors calcined at 950°C for 6 h in air are shown in Fig. 3. For $La_{0.97}Pr_{0.03}VO_4$ phosphor, there are two broad absorption peaks in the absorption spectrum from 200 to 350 nm, which correspond to the O^{2-} and V^{5+} charge transfer for the VO_4^{3-} internal anions [23-25]. The absorption band from 280 to 350 nm centered at 315 nm is attributed to the 4f-5d characteristic transition absorption of a Pr^{3+} ion because typical Pr^{3+}-activated oxide phosphors always demonstrate strong 4f-5d transition band absorption at approximately 200-330 nm [26-27]. There are small absorption peaks from 440 to 500 nm and 580 to 620 nm, respectively, which are corresponding to the inner 4f orbital characteristic transition of the Pr^{3+} ion. The different concentrations of Bi^{3+} ion do not affect the curves shape but do affect the intensities of the excitation and emission peaks.

Fig. 4 shows the excitation spectra for $(La_{0.97-y}Bi_y)Pr_{0.03}VO_4$ (y = 0-0.05) phosphor calcined at 950°C for 6 h in air. The signals are detected at 489 nm. There are two excitation bands in the excitation spectra. The first one from 200 to 350 nm centered at 315 nm is attributed to the charge transfer from the oxygen ligands to the central vanadium atom inside the VO_4^{3-}

anionic group, which overlaps the 4f-5d characteristic transition of the Pr^{3+} ion at the absorption band in $(La_{0.97-y}Bi_y)Pr_{0.03}VO_4$ phosphor. The other one centered at 448 nm is attributed to the $^3H_4 \rightarrow ^3P_2$ electronic transition of the Pr^{3+} ion inner 4f orbital [28].
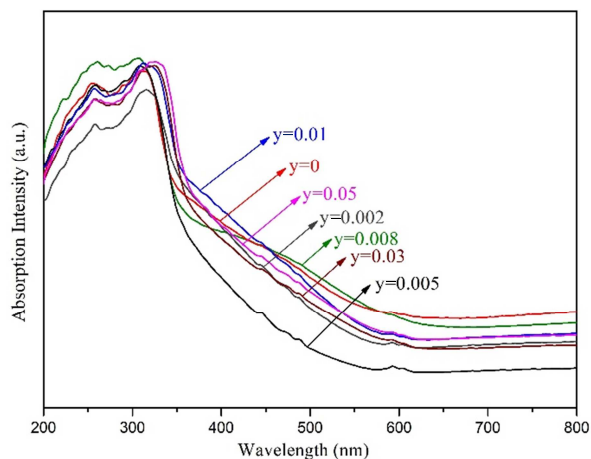
Fig. 3 Absorption spectra for $(La_{0.97-y}Bi_y)Pr_{0.03}VO_4$ phosphors that are calcined at 950°C for 6 h
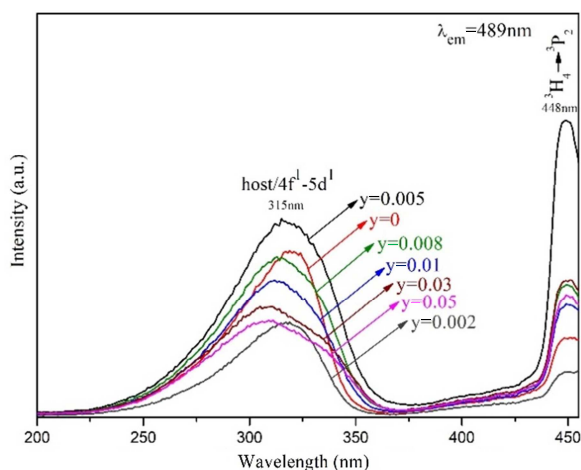
Fig. 4 Excitation spectra for $(La_{0.97-y}Bi_y)Pr_{0.03}VO_4$ phosphors that are calcined
at 950°C for 6 h (The signals are detected at 489 nm)

The intensity of the excitation peak increases significantly if $La_{0.97}Pr_{0.03}VO_4$ is doped with 0.5 mol% of Bi^{3+} ion and then decreases as the Bi^{3+} ion concentrations increases further. It is due to the extra absorption involving the Bi-O component in addition to the V-O charge transfer bands. In this study, the excitation wavelength is 315 nm, which is in good accordance with the $^1S_0 \rightarrow ^3P_1$ transition (A-band) for the electron level transition of Bi^{3+} ion [29]. Therefore, the role for Bi^{3+} ion-doped $La_{0.97}Pr_{0.03}VO_4$ phosphor in this study is to be a sensitizer. The excitation peak intensities are decreased when the Bi^{3+} ion concentration is higher than 0.5 mol%, because an increase in the Bi^{3+} ion concentration causes the phosphor particles to aggregate. It can dissipate the absorbed energy in the form of non-radiation rather than transfer it to the Pr^{3+} ions [30]. However, it can be observed that there is a blue shift for the excitation band from 320 nm to 308 nm as the Bi^{3+} ion contents increased. This may be the reason for the special empirical rule, that is substitutions of the dodecahedral La^{3+} by larger ions leading to spectral red shift and smaller ions leading to blue shift for most of the phosphor modification system [31].

Fig. 5 shows the emission spectra for $(La_{0.97-y}Bi_y)Pr_{0.03}VO_4$ phosphors calcined at 950°C for 6 h in air under an excitation of 315 nm. At 315 nm excitation, there is no emission peak of the Bi^{3+} ion observed in the emission spectra, but there are emission peaks in the visible light region at 480-520, 530-570, 580-610, 610-620, and 625-650 nm, which respectively correspond to the $^3P_0 \rightarrow ^3H_4$, $^3P_0 \rightarrow ^3H_5$, $^1D_2 \rightarrow ^3H_4$, $^3P_0 \rightarrow ^3H_6$, and $^3P_0 \rightarrow ^3F_2$ electron transitions of Pr^{3+} ions. The $^1D_2 \rightarrow ^3H_4$ transition is more intense than that for $^3P_0 \rightarrow ^3H_4$ at a low doping concentrations of Pr^{3+} ion (x = 0.005-0.02), but the intensity decreases if the Pr^{3+} ion concentration increases further (x = 0.03-0.1) [32]. It is due to the difference in the ionic radii of La^{3+}

ion and Pr^{3+} ion, which may compress the Pr-O bond in the host lattice when a slight Pr^{3+} ion concentration doped. This results in a strong crystal field effect causing the Stark splitting of the multiplet structure which leads the 4f-5d state of the Pr^{3+} ion to shifts to a lower energy state that is closer to the $^1D_2$ state, causing the emission intensities of the $^1D_2 \rightarrow ^3H_4$ transition to be higher than that of $^3P_0 \rightarrow ^3H_4$ transition. The results for this study show that the $^3P_0 \rightarrow ^3H_4$ transition is greater than the intensity of the $^1D_2 \rightarrow ^3H_4$ transition because the Pr^{3+} ion concentration is fixed of 3 mol%. Therefore, the CIE chromaticity coordinates are located in the white light region (x = 0.388, y = 0.367).
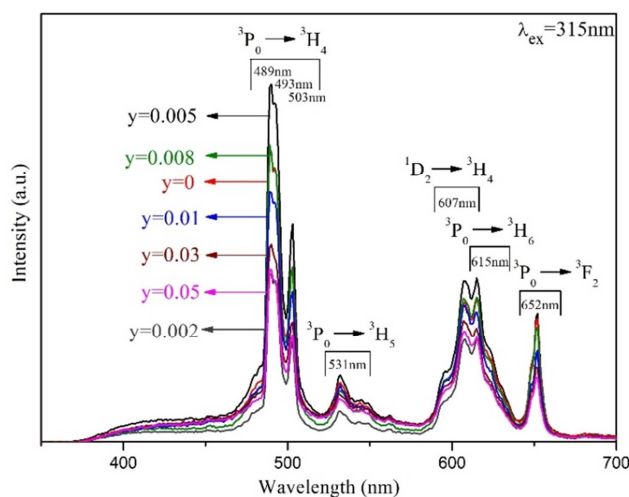
Fig. 5 Emission spectra for $(La_{0.97-y}Bi_y)Pr_{0.03}VO_4$ phosphors calcined
at 950°C for 6 h under an excitation of 315 nm

According to the results in the emission spectra, the intensity of emission peaks increases as the concentrations of Bi^{3+} ion in $La_{0.97}Pr_{0.03}VO_4$ phosphor increase. The co-doped with Bi^{3+} ions can increase an absorption in the ultraviolet region (315 nm) because the Bi^{3+} ion acts as a sensitizer in the $La_{0.97}Pr_{0.03}VO_4$ phosphor. A good sensitizer absorbs the excitation energy and transfers energy to a luminescent center (activator), but does not play a role as a luminescent or quenching center. More energy is absorbed and transferred to the Pr^{3+} ions via the Bi^{3+} ion, so the emission intensity of the $La_{0.97}Pr_{0.03}VO_4$ phosphor increases. There is a maximum intensity of emission peak when the Bi^{3+} ion concentration is 0.5 mol%. These results show that the sensitization effect of Bi^{3+} ion on the Pr^{3+} emission behavior varies with the Bi^{3+} ion concentrations.

As can be seen in the emission spectra, the emission peak appearances are attributing to the characteristic electronic transition of Pr^{3+} ion. There is no Bi^{3+} ion emission peak observed, because the Bi^{3+} acts as a sensitizer for doping in the $La_{0.97}Pr_{0.03}VO_4$ phosphor. The excitation wavelength, 315 nm, is not only absorbed by $LaVO_4$ host, but also absorbed by Bi^{3+} sensitizer and Pr^{3+} ion, respectively. The 4f-5d characteristics transition absorption of Pr^{3+} ion usually overlaps with the oxygen ligands to the central vanadium atom inside the VO_4^{3-} anionic group. Therefore, the energy (315 nm) is supposed firstly to be absorbed by the $LaVO_4$ host, Bi^{3+} ion, and the Pr^{3+} ion to the conduction band, the $^3P_1$ level, and the 4f-5d state, respectively. The energy in the 4f-5d state of Pr^{3+} ion relaxes to a lower state of $^3P_0$, and both of the energies in the conduction band and the $^3P_1$ level are all transferred to the 4f-5d state of the Pr^{3+} ion. Simultaneously, these energies from 4f-5d state relaxes rapidly to the lowest emission level, $^3P_0$ and $^1D_2$, via non-radiative transition, and finally transits from $^3P_0$ to the $^3H_{J, J=4, 5, 6}$ and the $^3F_2$ state, respectively, and from $^1D_2$ to $^3H_4$ state. The mechanism for energy absorption and transfer for $La_{0.97}Pr_{0.03}VO_4$ phosphor doped with Bi^{3+} ion is shown in Fig. 6.

Fig. 7 shows the CIE color coordinate diagrams for $(La_{0.97-y}Bi_y)Pr_{0.03}VO_4$ (y = 0-0.05) phosphors, y = 0.005, 0.01, 0.02, 0.03, 0.05, and 0.1. For the $La_{0.97}Pr_{0.03}VO_4$ phosphor with no Bi^{3+} ion doped, the emission color is in the near white light region with the CIE chromaticity coordinates of (x = 0.388, y = 0.367). For phosphors that are doped with Bi^{3+} ions, different concentrations of Bi^{3+} ion do not affect the shape of curves, but the intensity of the emission spectra changes. Therefore, the CIE color coordinates for $La_{0.97-y}Bi_yPr_{0.03}VO_4$ phosphor are all located in the near white light region.
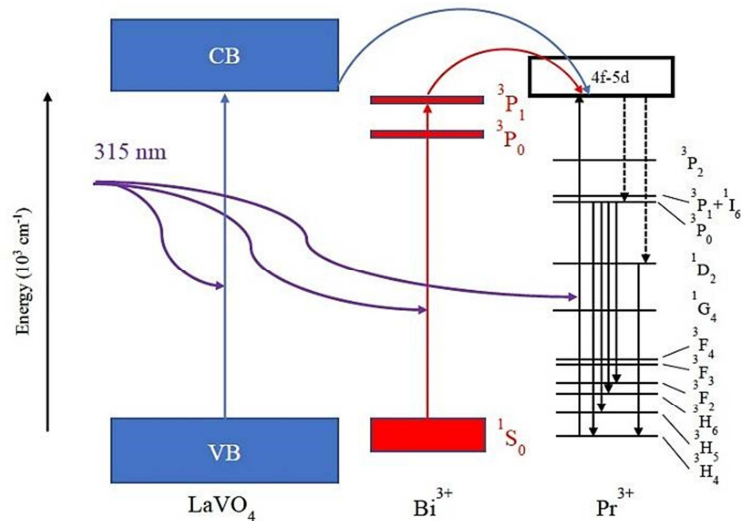
Fig. 6 The mechanism for the absorption of energy and transfer for $La_{0.97}Pr_{0.03}VO_4$ phosphors doped with Bi^{3+} ion under an excitation wavelength of 315 nm
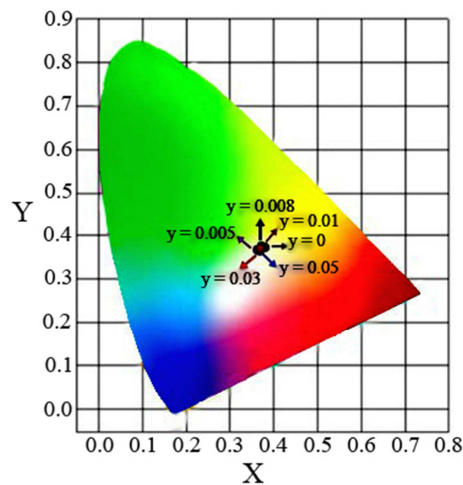
Fig. 7 CIE color coordinate diagrams for $(La_{0.97-y}Bi_y)Pr_{0.03}VO_4$ (y = 0-0.05) phosphor

4. Conclusions

The $(La_{0.97-y}Bi_y)Pr_{0.03}VO_4$ (y = 0-0.05) phosphors were synthesized using a sol-gel method at a calcination temperature of 950°C for 6 h in air. When doped with Bi^{3+} ions, the crystal structure of $(La_{0.97-y}Bi_y)Pr_{0.03}VO_4$ is monoclinic structure of $LaVO_4$, and there are no secondary phases. The surface morphologies of $(La_{0.97-y}Bi_y)Pr_{0.03}VO_4$ phosphors become smoother and more granular as the Bi^{3+} ion concentration increases. The role for a Bi^{3+} ion in the $La_{0.97}Pr_{0.03}VO_4$ phosphor system not only can be a flux, but also acts as a sensitizer. Under excitation at 315 nm, the emission intensity increases as the concentration of the Bi^{3+} ion increases. The phosphor emission has a maximum intensity at a Bi^{3+} ion concentration of 0.5 mol%. All of the CIE chromaticity coordinates of $(La_{0.97-y}Bi_y)Pr_{0.03}VO_4$ (y = 0-0.05) are located in the near white light region.

Acknowledgements

Conflicts of Interest

The authors declare no conflict of interest.

References

[1] H. Yie, S. Kim, Y. Kim, and H. S. Kim, "Modifying Optical Properties of Phosphor-in-Glass by Varying Phosphor Size and Content," Journal of Non-Crystalline Solids, vol. 463, pp. 19-24, May 2017.

[2] W. Dai, J. Hu, S. Shi, J. Zhou, K. Huang, S. Xu, et al., "Optical Properties of Aluminosilicate Phosphor for Lighting and Temperature Sensing," Journal of Luminescence, vol. 213, pp. 241-248, September 2019.

[3] A. Bergh, G. Craford, A. Duggal, and R. Haitz, "The Promise and Challenge of Solid-State Lighting," Physics Today, vol. 54, no. 12, pp. 42-47, December 2001.

[4] E. F. Schubert and J. K. Kim, "Solid-State Light Sources Getting Smart," Science, vol. 308, no. 5726, pp. 1274-1278, May 2005.

[5] S. Nakamura, M. Senoh, and T. Mukai, "High-Power InGaN/GaN Double-Heterostructure Violet Light Emitting Diodes," Applied Physics Letters, vol. 62, no. 19, pp. 2390-2392, May 1993.

[6] B. Yang, Z. Yang, Y. Liu, F. Lu, P. Li, Y. Yang, et al., "Synthesis and Photoluminescence Properties of the High-Brightness Eu^{3+}-Doped $Sr_3Y(PO_4)_3$ Red Phosphors," Ceramics International, vol. 38, no. 6, pp. 4895-4900, August 2012.

[7] K. Toda, Y. Kawakami, S. I. Kousaka, Y. Ito, A. Komeno, K. Uematsu, et al., "New Silicate Phosphors for a White LED," IEICE Transactions on Electronics, vol. 89-C, no. 10, pp. 1406-1412, October 2006.

[8] Y. Shimizu, K. Sakano, Y. Noguchi, and T. Moriguchi, Light Emitting Device Having a Nitride Compound Semiconductor and a Phosphor Containing a Garnet Fluorescent Material, U.S. Patent, 5,998,925, December 07, 1998.

[9] Y. Y. Tsai, H. R. Shih, M. T. Tsai, and Y. S. Chang, "A Novel Single-Phased White Light Emitting Phosphor of Eu^{3+} Ions-Doped Ca_2LaTaO_6," Materials Chemistry and Physics, vol. 143, no. 2, pp. 611-615, January 2014.

[10] X. Liu, C. Lin, and J. Lin, "White Light Emission from Eu^{3+} in $CaIn_2O_4$ Host Lattices," Applied Physics Letters, vol. 90, no. 8, 081904, February 2007.

[11] W. Fan, X. Song, S. Sun, and X. Zhao, "Microemulsion-Mediated Hydrothermal Synthesis and Characterization of Zircon-Type $LaVO_4$ Nanowires," Journal of Solid State Chemistry, vol. 180, no. 1, pp. 284-290, January 2007.

[12] W. Fan, W. Zhao, L. You, X. Song, W. Zhang, H. Yu, et al., "A Simple Method to Synthesize Single-Crystalline Lanthanide Orthovanadate Nanorods," Journal of Solid State Chemistry, vol. 177, no. 12, pp. 4399-4403, December 2004.

[13] A. B. Meggy, B. L. Tonge, and R. A. Williams, "Cobalt Complexes of Polyglycines," Nature, vol. 198, pp. 1084-1085, June 1963.

[14] Y. Terada, K. Shimamura, V. V. Kochurikhin, L. V. Barashov, M. A. Ivanov, and T. Fukuda, "Growth and Optical Properties of $ErVO_4$ and $LuVO_4$ Single Crystals," Journal of Crystal Growth, vol. 167, no. 1-2, pp. 369-372, September 1996.

[15] A. Huignard, T. Gacoin, and J. P. Boilot, "Synthesis and Luminescence Properties of Colloidal YVO_4: Eu Phosphors," Chemistry of Materials, vol. 12, no. 4, pp. 1090-1094, March 2000.

[16] H. L. Chen, L. K. Wei, and Y. S. Chang, "Characterizations of Pr^{3+} Ion-Doped $LaVO_4$ Phosphor Prepared Using a Sol-Gel Method," Journal of Electronic Materials, vol. 47, no. 11, pp. 6649-6654, November 2018.

[17] H. Terraschke and C. Wickeder, "UV, Blue, Green, Yellow, Red, and Small: Newest Developments on Eu^{2+}-Doped Nanophosphors," Chemical Reviews, vol. 115, no. 20, pp. 11352-11378, October 2015.

[18] Y. S. Chang, H. R. Shih, M. T. Tsai, K. T. Liu, and L. G. Teoh, "Photoluminescence Properties of La^{3+}-Doped $BaY_{1.94}Eu_{0.06}ZnO_5$ Phosphor Prepared Using a Sol-Gel Method," Journal of Luminescence, vol. 157, pp. 98-103, January 2015.

[19] W. Dörr, H. Assmann, G. Maier, and J. Steven, "Bestimmung der Dichte, Offenen Porosität, Porengrössenverteilung und Spezifischen Oberflache von UO_2-Tabletten," Journal of Nuclear Materials, vol. 81, no. 1-2, pp. 135-141, April 1979.

[20] C. H. Liang, Y. C. Chang, and Y. S. Chang, "Enhancement of Luminescent Properties by Sr^{2+} Substituting Ba^{2+} in Red-Emitting Phosphors: $Ba_{1-y}Sr_yLa_{2-x}ZnO_5$: xEu (x=0-1, y=0-0.7)," Journal of the Electrochemical Society, vol. 156, no. 10, J303, January 2009.

[21] G. Blasse and B. C. Grabmaier, Luminescent Materials, Berlin: Springer-Verlag Berlin Heidelberg, 1994.

[22] S. Shionoya, W. M. Yen, and H. Yamamoto, Phosphor Handbook, 2nd ed. United States: CRC Press, 2006.

[23] K. A. Gschneidner, J. C. G. Bünzli, and V. K. Pecharsky, Handbook on the Physics and Chemistry of Rare Earths, United Kingdom: Elsevier B. V., 2011.

[24] C. Hsu and R. C. Powell, "Energy Transfer in Europium Doped Yttrium Vanadate Crystals," Journal of Luminescence, vol. 10, no. 5, pp. 273-293, June 1975.

[25] H. Zhang, X. Fu, S. Niu, G. Sun, and Q. Xin, "Photoluminescence of YVO$_4$: Tm Phosphor Prepared by a Polymerizable Complex Method," Solid State Communications, vol. 132, no. 8, pp. 527-531, November 2004.

[26] C. D. M. Donega, A. Meijerink, and G. Blasse, "Non-Radiative Relaxation Processes of the Pr^{3+} Ion in Solids," Journal of Physics and Chemistry of Solids, vol. 56, no. 5, pp. 673-685, May 1995.

[27] H. Hoefdraad and G. Blasse, "Green Emitting Praseodymium in Calcium Zirconate," Physica Status Solidi (A), vol. 29, no. 1, pp. K95-K97, May 1975.

[28] V. R. Prasad, S. Damodaraiah, S. N. Devara, and Y. C. Ratnakaram, "Photoluminescence Studies on Holmium (III) and Praseodymium (III) Doped Calcium Borophosphate (CBP) Phosphors," Journal of Molecular Structure, vol. 1160, no. 15, pp. 383-392, May 2018.

[29] X. Wang, J. Wang, X. Li, H. Luo, and M. Peng, "Novel Bismuth Activated Blue-Emitting Phosphor Ba$_2$Y$_5$B$_5$O$_{17}$: Bi^{3+} with Strong NUV Excitation for WLEDs," Journal of Materials Chemistry C, vol. 7, no. 36, pp. 11227-11233, September 2019.

[30] M. Puchalska, E. Zych, and P. Bolek, "Luminescences of Bi^{3+} and Bi^{2+} Ions in Bi-Doped CaAl$_4$O$_7$ Phosphor Powders Obtained via Modified Pechini Citrate Process," Journal of Alloys and Compounds, vol. 806, no. 25, pp. 798-805, October 2019.

[31] J. Zhong, W. Zhao, W. Zhuang, W. Xiao, Y. Zheng, F. Du, et al., "Origin of Spectral Blue Shift of Lu^{3+}-Codoped YAG:Ce^{3+} Phosphor: First-Principles Study," ACS Omega, vol. 2, no. 9, pp. 5935-5941, September 2017.

[32] L. G. Teoh, M. T. Tsai, Y. C. Chang, and Y. S. Chang, "Photoluminescence Properties of Pr^{3+} Ion-Doped YInGe$_2$O$_7$ Phosphor under an Ultraviolet Irradiation," Ceramics International, vol. 44, no. 3, pp. 2656-2660, February 2018.